

**Project: COLLABORATIVE RESEARCH: STUDY OF AEROSOL SOURCES AND
PROCESSING AT THE GVAX PANTNAGER SUPERSITE (PI: Doug Worsnop)**

Final report by Co-PI: Rainer Volkamer, University of Colorado at Boulder

Executive Summary

The Two Column Aerosol Project (TCAP) investigated uncertainties in the aerosol direct effect in the northern hemisphere mid-latitudes. The University of Colorado 2D-MAX-DOAS and LED-CE-DOAS instruments were collocated with DOE's Atmospheric Radiation Measurement (ARM) Mobile Facility (AMF) and Mobile Aerosol Observing System (MAOS) during the TCAP-1 campaign at Cape Cod, MA (1 July to 13 August 2012).

We have performed atmospheric radiation closure studies to evaluate the use of a novel parameter, i.e., the Raman Scattering Probability (RSP). We have performed first measurements of RSP almucantar scans, and measure RSP in spectra of scattered solar photons at 350nm and 430nm. Radiative Transfer Modelling of RSP demonstrate that the RSP measurement is maximally sensitive to infer even extremely low aerosol optical depth ($AOD < 0.01$) reliably by DOAS at low solar relative azimuth angles. We further assess the role of elevated aerosol layers on near surface observations of oxygen collision complexes, O_2-O_2 . Elevated aerosol layers modify the near surface absorption of O_2-O_2 and RSP. The combination of RSP and O_2-O_2 holds largely unexplored potential to better constrain elevated aerosol layers and measure column aerosol optical properties such as aerosol effective radius, extinction, aerosol phase functions and refractive indices.

The TCAP deployment also provides a time series of reactive trace gas vertical profiles, i.e., nitrogen dioxide (NO_2) and glyoxal ($C_2H_2O_2$), which are measured simultaneously with the aerosol optical properties by DOAS. NO_2 is an important precursor for ozone (O_3) that modifies oxidative capacity. Glyoxal modifies oxidative capacity and is a source for brown carbon by forming secondary organic aerosol (SOA) via multiphase reactions in aerosol and cloud water. We have performed field measurements of these gases during TCAP, and conducted laboratory experiments to quantify for the first time the Setschenow salting constant, K_S , of glyoxal in sulfate aerosols. Knowledge about K_S is prerequisite to predict how increasing sulfate concentrations since pre-industrial times have modified the formation of SOA from biogenic gases in atmospheric models.

We have performed the following activities:

- ❑ The University of Colorado 2D scanning ground Multi AXis Differential Optical Absorption Spectroscopy (2D-GMAX-DOAS) and LED Cavity Enhanced DOAS (LED-CE-DOAS) instruments were deployed from 1 July until 13 August 2012 at Cape Cod, MA as part of the two Column Aerosol Project (TCAP). TCAP investigates uncertainties in the aerosol direct effect in the northern hemisphere mid-latitudes. The 2D-GMAX-DOAS and LED-CE-DOAS were collocated with DOE's Atmospheric Radiation Measurement (ARM) Mobile Facility (AMF) and Mobile Aerosol Observing System (MAOS) to 1) perform atmospheric radiation closure studies to evaluate the use of a novel parameter, i.e., the Raman Scattering Probability (RSP), to measure extremely low aerosol optical depth ($AOD < 0.01$) reliably by DOAS, and 2) assess the role of elevated aerosol layers on near surface observations of oxygen collision complexes, O_2-O_2 . In addition we have performed simultaneous measurements of aerosol optical properties and various reactive trace gases, and used TCAP data to verify the validity of DOAS retrievals of the column effective radius and refractive index of aerosols.
- ❑ The retrieval algorithms developed here were applied to measure nitrogen dioxide (NO_2) and glyoxal ($C_2H_2O_2$) during TCAP, and accomplish the first detection of iodine oxide (IO) in the tropical free troposphere by means of the CU Airborne MAX-DOAS instrument.
- ❑ The award provided data analysis time for simulation chamber experiments of secondary organic aerosol (SOA) formation from glyoxal at the Paul Scherrer Institute (PSI) in Switzerland (Kampf et al., 2013, *ES&T*), and the application of these laboratory measurements to predict SOA by atmospheric models in Mexico City (Waxman et al., 2013, *GRL*), and over the continental US (Knote et al., 2014, *ACP*).

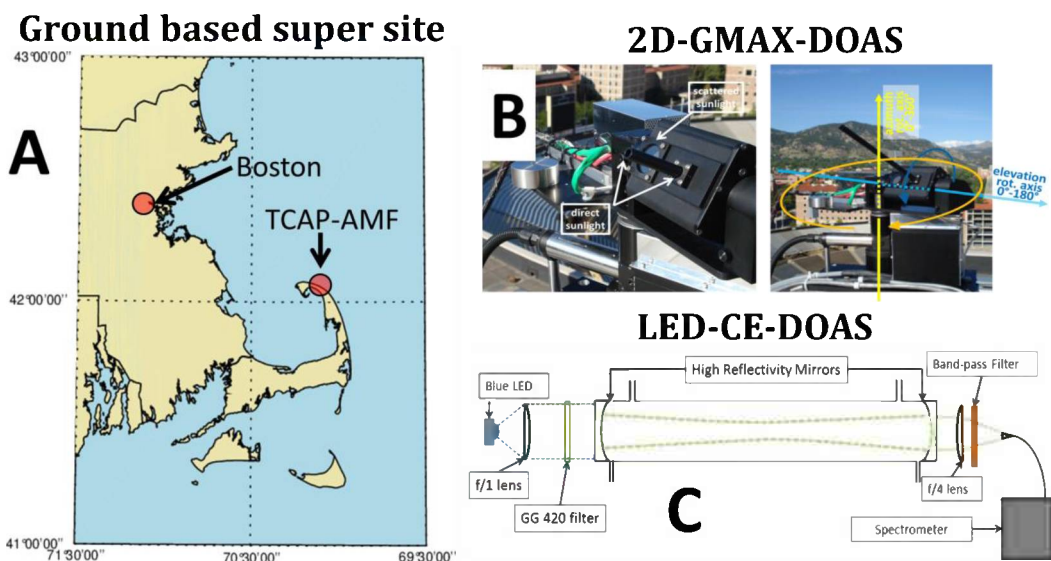


Figure 1: The 2D-GMAX-DOAS (B) and LED-Cavity Enhanced DOAS (LEC-CE-DOAS) (C) instruments were deployed at the AMF site (A) from 1 Jul – 13 Aug 2012.

Notable Events & Highlights:

1) Radiation Closure Study under conditions of low AOD

- ❑ The 2D-MAX-DOAS deployment during TCAP provided an opportunity to evaluate innovative retrievals of very low AOD by DOAS measurements of the Raman Scattering Probability (RSP). RSP measurements are based on the quantitative interpretation of the Ring effect, i.e, the filling-in of Fraunhofer lines due to Rotational Raman Scattering. We have measured the RSP in the UV (350nm) and visible (430nm) spectral range. Example fits that were measured on 22 July 2012 during TCAP are shown in Figure 2.
- ❑ RSP retrievals are inherently calibrated, and do not require an external calibration source. They are based exclusively on measurements of relative intensity changes in hyperspectral measurements of scattered solar radiation at different solar relative azimuth angles (SRAA, see Figure 2). This significantly reduces instrument maintenance, and facilitates autonomous operation in remote locations, and more robust retrievals of aerosols even at very low AOD. Simultaneously also the trace gases trace gases nitrogen dioxide (NO₂), formaldehyde (HCHO), glyoxal (CHOCHO) and oxygen dimers (O₂-O₂) can be measured selectively by means of a single instrument.

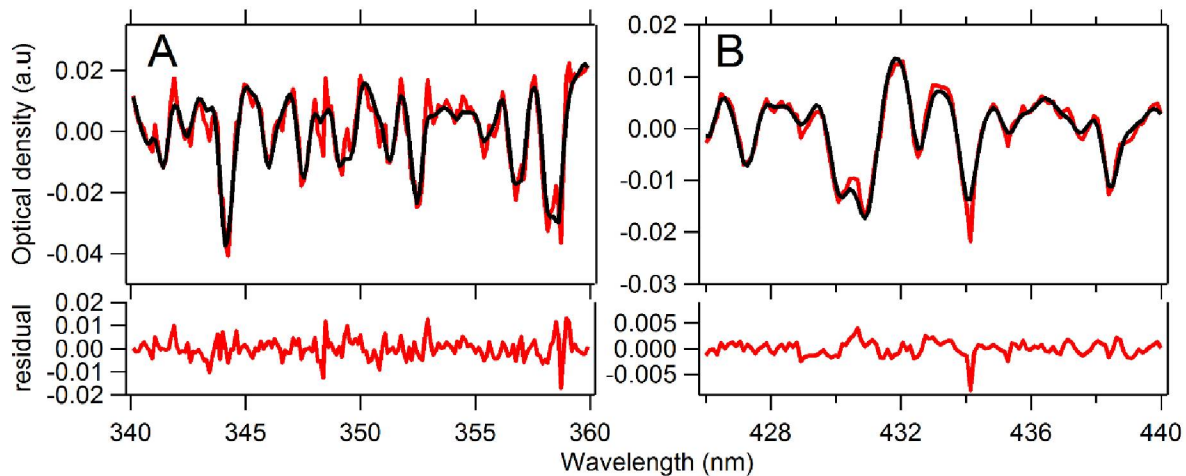


Figure 2: Example of spectral proofs for the detection of RSP in the UV (A) and visible (B) on 22 July 2012 at $\theta_0 = 76.5^\circ$ during the TCAP field campaign. The red lines represent the measured spectra and black lines are fitted Ring reference cross sections. The fit examples shown here are for an EA = 1° and the RSP obtained are 0.090 (RMS = 4.4×10^{-3}) and 0.051 (RMS = 1.0×10^{-3}) for the UV and visible respectively (see text for details).

- ❑ For the first time to our knowledge, we analyze RSP from spectra recorded with the solar almucantar scan. Radiative transfer simulations (RTM) of the RSP indicate that decreases for angles close to the sun and responds most strongly at low AOD. We carried out further sensitivity studies to investigate the influence of several important input parameters in the simulations of the RSP when using a typical solar almucantar scan. Figure 3 shows the main findings. Even very small changes of AOD (~ 0.005) have a strong effect in the RSP signal, especially for angles close to the sun ($-50^\circ < \text{SRAA} < 50^\circ$) (yellow area in Figure 3). Previous RSP measurements have only been conducted for elevation angle scans (Wagner et

al. 2009b; Wagner et al. 2010). Figure 3 demonstrates that RSP almucantar scans show the greatest potential to quantitatively infer low AOD at low SRAA.

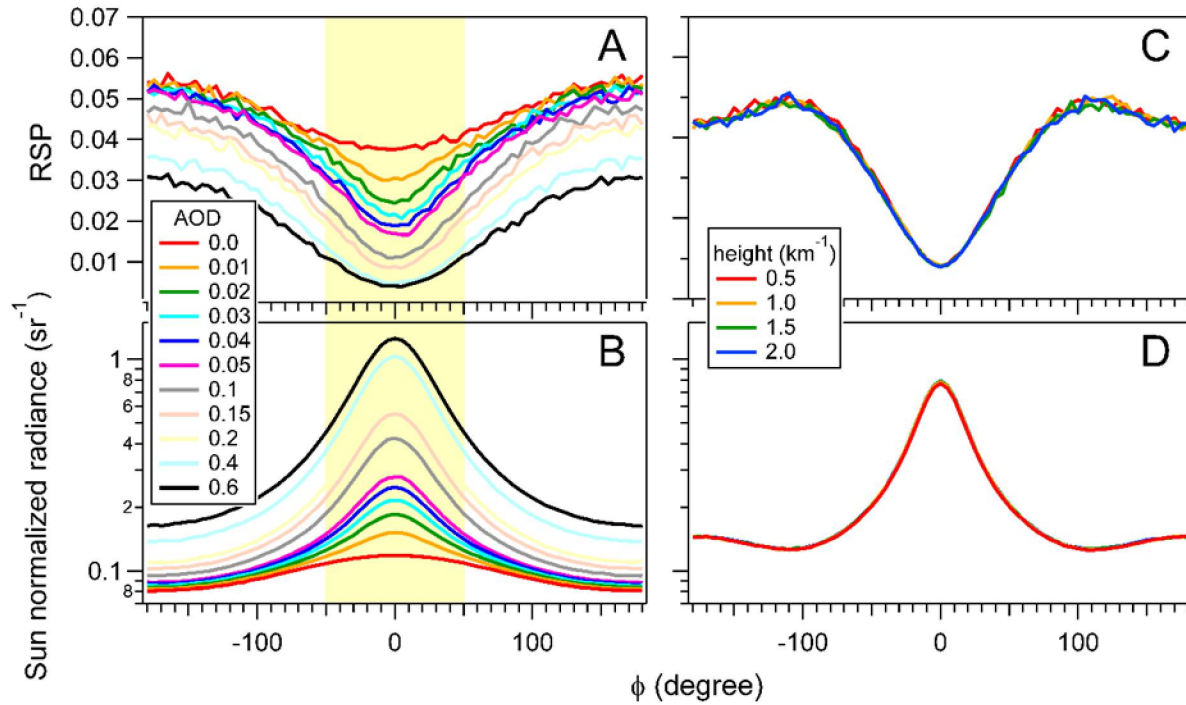


Figure 3: Sensitivity study of simulated RSP and sun normalized radiances using the solar relative azimuth scan (430 nm). The effect of several AODs with fixed aerosol box height (1.5 km) are shown in figures A and B for the RSP and radiances respectively. The effect of box aerosol heights with fixed AOD of 0.2 are shown in figures C and D for the RSP and radiances respectively. The simulation is at $\text{SZA} = 35^\circ$ (additional input properties are $\text{SSA} = 0.98$, $g = 0.70$, $\text{SA} = 0.05$). The yellow region represent the angles where maximum sensitivity is achieved for small changes of AOD.

- ☐ We evaluate our RSP-based AOD retrieval based on the solar almucantar scan using independent measurements of AOD from a co-located Cimel sun photometer (Figure 4).

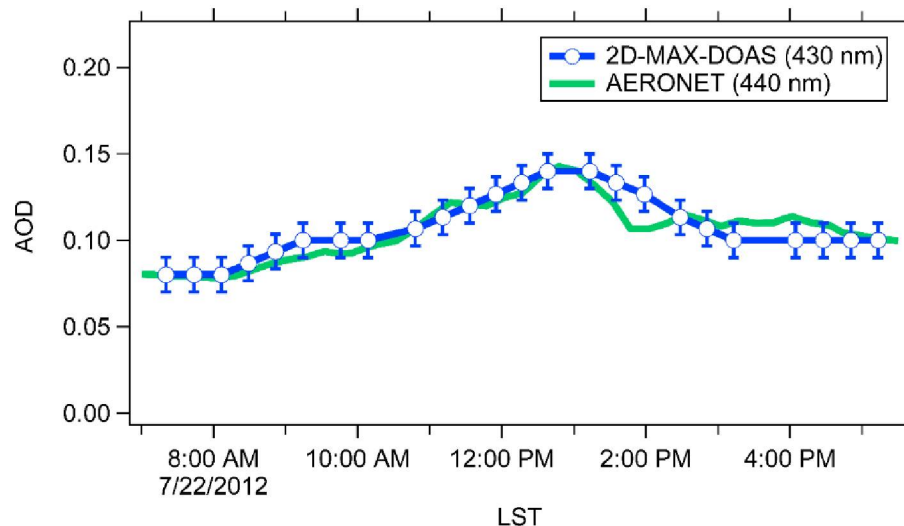


Figure 4: Comparison of AOD retrieved with the 2D-MAX-DOAS and the co-located Cimel Sun photometer on 22 July (near Rayleigh scattering conditions).

2) DOAS measurements of aerosol microphysical properties

- ❑ The retrieval strategy to estimate the aerosol microphysical properties described in Ortega et al. (2015) was applied on 17 and 22 July 2012, and selected results are presented here. Fig 5A shows the comparison between the DOAS retrieved column effective radius of aerosol with those measured on-board the G-1 aircraft. A remarkably consistency of the retrieved column effective radius is observed: $R_{e,DOAS} = 0.19 \pm 0.025 \mu\text{m}$; in-situ $R_{e,G1} = 0.18 \pm 0.014 \mu\text{m}$, and $R_{e,HSRL-2} = 0.18 \mu\text{m}$. The remarkably good agreement with two independent instruments show that almucantar measurements with 2-D-MAX-DOAS are reliable to estimate effective particle radius and should be considered in closure studies in future deployments.
- ❑ Figure 5B presents the average effective real part of the refractive index (n). In this case, the retrieval inversion captures a significant wavelength dependence between the UV and visible wavelengths. The visible wavelength (450 – 560 nm) are merged to construct a single n with an average of 1.54 ± 0.04 , while at 350 the average n is 1.40 ± 0.02 . The uncertainty is estimated with the standard error of the mean. The real part of the refractive index describes the scattering properties of the aerosol and is related directly to the parameterized aerosol phase function g in the Mie calculations.
- ❑ Fig. 5C shows the wavelength dependence of the aerosol phase function, g . As expected, g is larger for shorter wavelengths indicating stronger preference in the scattering forward direction. The variability in the retrieval of the imaginary part of refractive index is higher and contains higher uncertainties, however the values are consistently lower than 0.01 for all wavelengths. The low values of k indicates that during this period the absorption of aerosols is low, resulting in a single scattering albedo larger than 0.96 for all wavelengths. A quantitative validation of such low complex refractive index is challenging. Kassianov et al. (2014) presented a method for retrieving simultaneously the effective density and real refractive index using in-situ measurements during TCAP. The authors applied their approach on weakly absorbing aerosol in agreement with our findings in this work. The mean and standard deviation of the retrieved effective real refractive index for wet and dry sub-micron particles at 550 nm was 1.487 ± 0.022 , which is slightly lower than our estimated average column refractive index in the visible of 1.54 but within the estimated uncertainty. The cause of the small differences might be related to differences in sensitivity on air masses and/or aerosol water effects. Our method is applied to the whole aerosol column and does not distinguish wet and dry conditions while the in-situ method is sensitive to localized air masses and correction for water uptake needs to be considered. Unfortunately Kassianov et al. (2014) does not present results at different wavelengths.
- ❑ The complex refractive index depends primary on the particle composition, hence an additional way to assess our findings is through calculations of the refractive index based on mixing rules. The aerosol chemical composition during the TCAP campaign is examined in more detail in Berg et al. (2015). On 17 July before 13 LST (same time as our retrieved properties), the organics accounted on average 69 % of the mass fraction of non-refractory particles. Sulfates (SO_4) accounted for 19.6 %, ammonium (NH_4) accounted for 8.1% and nitrates (NO_3) with 3.3% to the mass fraction. During the low approach of the G-1 the mass fraction was similar as on the ground, however differences in air mass loading along altitude

was identified (for details see Berg et al. (2015)). We apply the volume-weighted method to calculate the refractive index (m) using ρ and n (in parenthesis) as follows: 1.8 (1.52), 1.8 (1.5), and 1.8 (1.5) for SO_4 , NO_3 , and NH_4 respectively. Based on the weak absorbing results we assume that the organics to be purely scattering with a refractive index of 1.55 and density of $1.40 \text{ g}\cdot\text{cm}^{-3}$. The calculated volume weighted n is equal to 1.54, which agrees very well with our 1.54 ± 0.04 .

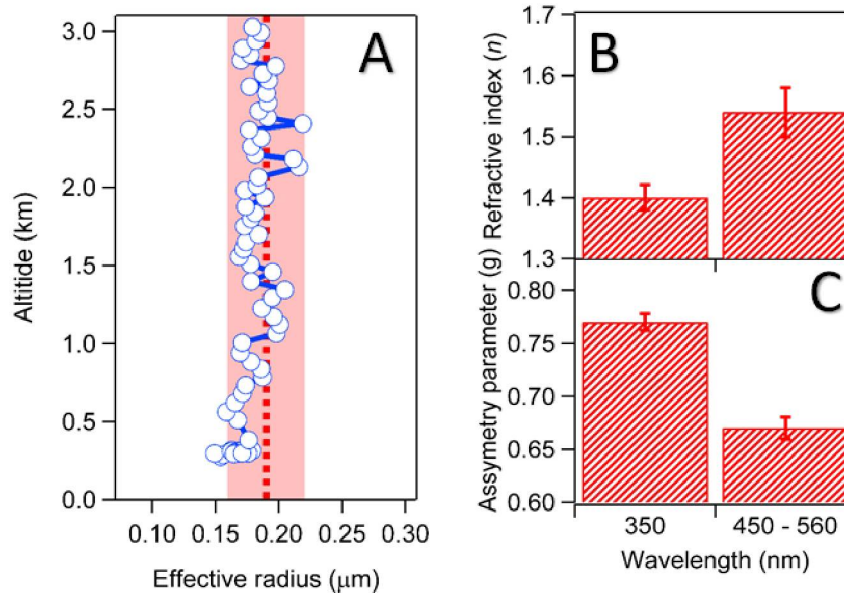


Figure 5: Results of the aerosol microphysical properties on July 17 2012. A: Comparison of the column r_e (dotted line) retrieved with the MAX-DOAS with the constructed r_e profile obtained during the G-1 low approach above the AMF ground site (blue circles). B: Wavelength dependence on the effective real part of the refractive index. C: The resulted wavelength asymmetry parameter resulted from the retrieval approach.

3) Elevated aerosol layers explain the apparent $\text{O}_2\text{-O}_2$ absorption during TCAP

- The oxygen collisional complex ($\text{O}_2\text{-O}_2$, or O_4) is a greenhouse gas, and a ubiquitous tracer molecule that informs about aerosol and cloud properties, and their effect on modifying the radiation state of the atmosphere. $\text{O}_2\text{-O}_2$ provides a calibration trace gas to infer photon path distributions with Differential Optical Absorption Spectroscopy (DOAS). An increasing number of reports have found the need for an $\text{O}_2\text{-O}_2$ correction factor (CFO_4) when comparing simulated and measured $\text{O}_2\text{-O}_2$ differential slant column densities (dSCD) by passive remote sensing DOAS. In this work, we investigate the sensitivity of $\text{O}_2\text{-O}_2$ dSCD simulations towards separately measured aerosol extinction profiles, and compare the simulations with measurements of $\text{O}_2\text{-O}_2$ dSCDs at ultra-violet (360 nm) and visible (477 nm) wavelengths.
- The measurements were conducted by the CU 2-D-MAX-DOAS instrument and NASA's multispectral High Spectral Resolution Lidar (HSRL-2) as part of the Two Column Aerosol Project (TCAP) in July 2012 at Cape Cod, MA under conditions of (1) high aerosol load (17

July 2012, aerosol optical depth, AOD ~ 0.35 at 477 nm) and (2) near molecular scattering conditions (22 July 2012, AOD < 0.10 at 477 nm).

- The measured and calculated O₂-O₂ dSCDs agreed within 6.4 ± 0.4 % (360 nm) and 4.7 ± 0.6 % (477 nm) if the HSRL-2 profiles were used as input to the calculations. However, if the aerosol extinction profile is confined to the surface (while keeping AOD constant) the CFO₄ was needed ($0.53 < \text{CFO}_4 < 0.75$), and in the range of previously reported CFO₄. Our results suggest that the need for CFO₄ is related to negative bias in the simulated O₂-O₂ dSCDs that is caused by ignoring elevated aerosol layers. The aerosol profile above the boundary layer needs to be taken into account when interpreting the O₂-O₂ from ground based MAX-DOAS. O₂-O₂ observations by ground-based MAX-DOAS are sensitive to elevated aerosol layers, and can provide opportunities to identify and better characterize these layers.

4) Time series of in-situ CHOCHO and NO₂ were measured by the CU LED-CED-DOAS instrument (Thalman and Volkamer 2010) at the TCAP ground site, and is shown in Fig 6.

- This data is currently being used by Dr. Jerome Fast for predictions of brown carbon SOA formation and effects on radiation using WRF-Chem.

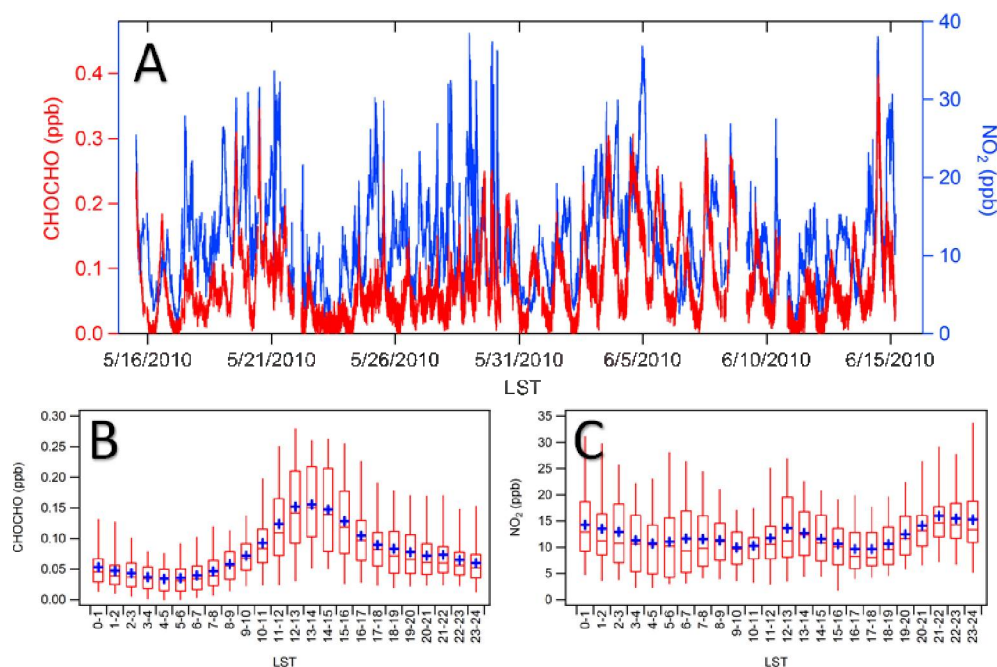


Figure 6: A: Time series of CHOCHO and NO₂ obtained with the in-situ CE-DOAS instrument at the TCAP ground site. The bottom plots show the diurnal profiles of CHOCHO (A) and NO₂ (B). Box and whisker plot: horizontal bar represents the median, the box represents the 25th and 75th percentiles, and the whiskers represents the 5th and 95th percentiles.

5) Detection of iodine oxide in the tropical free troposphere (Dix et al., 2013, PNAS)

- ❑ Atmospheric iodine monoxide (IO) is a radical that catalytically destroys heat trapping ozone and reacts further to form aerosols. The retrievals developed with support from this award have been applied to spectra recorded during the maiden flight of the CU Airborne MAX-DOAS instrument aboard the NSF/NCAR GV aircraft in Jan 2010 over the Central Pacific Ocean. We accomplished the first detection of IO in the tropical free troposphere (FT).
- ❑ Our measurements support that iodine recycles from aerosols back to the gas-phase as a result of heterogeneous chemical reactions. Chemical model simulations reveal that the iodine-induced ozone loss occurs mostly above the marine boundary layer (34%), in the transition layer (40%) and FT (26%) and accounts for up to 20% of the overall tropospheric ozone loss rate in the upper FT. The halogen-driven ozone loss in the FT is currently underestimated by atmospheric models and climate models.
- ❑ The results were published as Dix et al., 2013 *Proceedings of the National Academy of Sciences*.

6) Simulation chamber experiments of SOA formation from glyoxal

- ❑ Glyoxal, the smallest alpha-dicarbonyl, is a ubiquitous component of ambient aerosols in biogenic, urban, arctic, and marine atmospheres. It is generally believed that multiphase chemical reactions in cloud or aerosol water form soluble products with lower vapor pressures, and that this lowering of the vapor pressure is the primary cause for the enhanced partitioning.
- ❑ We have conducted laboratory experiments that show that this increased partitioning of glyoxal is due to electrostatic forces instead. We have quantified for the first time the time-resolved evolution of glyoxal partitioning to aqueous model aerosols containing sulfate. These measurements show an exponential increase in Henry's law constants with seed particle salt concentrations. This exponential increase is found to be independent of the presence or absence of organics in the seed particles, and can be explained by means of a single parameter, the Setschenow salting constant, K_S , to predict the partitioning of glyoxal over a wide range of environmental conditions (cloud water and concentrated salt solutions of aerosol water) (Kampf et al., 2013).
- ❑ Quantum chemical calculations show that glyoxal forms a surprisingly strong bond with sulfate ions. These hydrogen bounded complexes effectively displace water molecules from the hydration shell of sulfate ions, increasing the abundance of glyoxal as a building block for SOA formation in aerosol water compared to cloud water (Kurten et al., 2014).
- ❑ We present an equation to represent Setschenow salting-in and the subsequent SOA formation via multiphase reactions in atmospheric models. First applications in box-models and 3D chemical transport models suggest a significant contribution of sulfate to enhance the SOA formation from biogenic VOC (Waxman et al., 2013; Knöbe et al., 2014).

Publications from this project (authors from the Volkamer group are highlighted):

- ❑ Berg, L. et al., The Two-Column Aerosol Project: Phase I Overview and Impact of Elevated Aerosol Layers on Aerosol Optical Depth. *Journal of Geophysical Research - Atmospheres*, 2015, submitted.
- ❑ **Dix, B., S. Baidar**, J.F. Bresch, S.R. Hall, K.S. Schmidt, **S. Wang**, and **R. Volkamer** (2013). Detection of Iodine Monoxide in the Tropical Free Troposphere. *Proceedings of the National Academy of Sciences*, in press. doi: 10.1073/pnas.1212386110.
- ❑ **Kampf, C.J., E.M. Waxman**, J.G. Slowik, J. Dommen, L. Pfaffenberger, A.P. Praplan, A.S.H. Prevot, U. Baltensperger, T. Hoffmann, and **R. Volkamer**. [Effective Henry's Law Partitioning and the Salting Constant of Glyoxal in Aerosols Containing Sulfate](#), 2013, *Environmental Science and Technology*, 47(9), 4236-4244, doi: 10.1021/es400083d.
- ❑ Knote, C., A. Hodzic, J.L. Jimenez, **R. Volkamer**, J.J. Orlando, **S. Baidar**, J. Brioude, J. Fast, D.R. Gentner, A.H. Goldstein, P.L. Hayes, W.B. Knighton, **H. Oetjen**, A. Setyan, H. Stark, **R. Thalman**, G. Tyndall, R. Washenfelder, **E. Waxman**, and Q. Zhang. Simulation of Semi-explicit Mechanisms of SOA Formation from Glyoxal in a 3-D Model. 2014, *Atmospheric Chemistry and Physics*, 14, 6213-6239, doi:10.5194/acp-14-6213-2014
- ❑ Kurtén, T, J. Elm, N. Prisle, K. Mikkelsen, **C. Kampf, E. Waxman**, and **R. Volkamer**, A computational study of the effect of glyoxal – sulfate clustering on the Henry's law coefficient of glyoxal. 2014, *Journal of Physical Chemistry*, doi: 10.1021/jp510304c.
- ❑ **Ortega, I., Koenig, T., Sinreich, R., Thomson, D., and Volkamer, R.**: The CU 2-D MAX-DOAS instrument – Part 1: 3-D Retrieval of NO₂ and azimuth dependent OVOC ratios, *Atmos. Meas. Tech.*, 8, 2371-2395, 2015. doi: 10.5194/amt-8-2371-2015.
- ❑ **Ortega, I.**, L. Berg, R. Ferrare, J. Hair, C. Hostetler, T. Wagner, and **R. Volkamer**, Elevated aerosol layers modify the apparent O₂-O₂ absorption as seen by ground based MAX-DOAS, *Journal of Quantitative Spectroscopy and Radiative Transfer*, 2015, submitted.
- ❑ **Waxman, E.M.**, K. Dzepina, B. Ervens, J. Lee-Taylor, B. Aumont, J.L. Jimenez, S. Madronich, and **R. Volkamer**. Secondary Organic Aerosol Formation from Semi- and Intermediate- Volatility Organic Compounds and Glyoxal: Relevance of O/C as a Tracer for Aqueous Multiphase Chemistry. 2013, *Geophysical Research Letters*, doi: 10.1029/2012GL052871.